

## Research on Longitudinal Stiffness Modeling of Contact Metro Obstacle Detection Device

QIAN Ru<sup>1,a,\*</sup>, LI Yongmei<sup>1,b</sup>, ZHANG Weifen<sup>1,c</sup>

<sup>1</sup>Southeast University Chengxian College, Nanjing, China. 210088

<sup>a</sup> email: 715216392@qq.com, <sup>b</sup> email: 149687158@qq.com, <sup>c</sup> email: 11376714@qq.com

\*corresponding author: QIAN Ru

**Keywords:** Stiffness; Equivalent Modeling; Special-shaped Plate Spring; Contact Obstacle Detection Device

**Abstract:** Due to the non-linear stiffness of the contact Metro obstacle detection device, the research of structural mechanical properties and the theory of calculation model are not perfect. The working principle of the detection device was studied, the longitudinal stiffness of the whole structure is calculated by the load-maximum deformation equivalent of the special-shaped plate spring, the influence of assembly connection between parts in current calculation and analysis was evaded, so a new method for calculating the longitudinal load deformation of the device is provided. The results show that before the deformation of the spring is not obvious, the load deformation law based on the equivalent model is consistent with the experimental results, and the maximum error is less than 10%. So the equivalent modeling method of the longitudinal stiffness of the detection device has good feasibility and accuracy, and can meet the engineering needs.

### 1. Introduction

Subway obstacle detection device is widely used because of its significant improvement of urban rail traffic collision safety [1-2]. Wang Wei and others [3] have designed and tested an automatic recognition system for train obstacles based on video image recognition technology. Fang Chongquan [4] realized the obstacle detection with the two-dimensional scanning laser radar, which can recognize the obstacle and the terrain. Liu Hangdong and others [5] found through the study of intelligent driving architecture, obstacle detection algorithm flaws will directly lead to abnormal driving, and even traffic accidents. Yao Yuan and others [6] analyzed the advantages and disadvantages of mechanical contact and obstacle detection device based on image forming technology, and discussed the configuration scheme of auxiliary train driver driving system including obstacle detection. Subway tracks are mostly underground tunnels, and the traditional visual and radar detection of obstacles are inevitably missed due to the influence of light, signals, etc [7-8]. Therefore, the mechanical contact type obstacle detection device is indispensable for the subway operation, and provides an additional guarantee for its safe operation.

Based on the theory of bending deformation of cantilever beam, the working principle of contact obstacle detection device is studied, the stiffness model of the whole structure is established based on the Longitudinal load-deformation law of the abnormality leaf spring, and the feasibility and accuracy of the evaluation method of the detector are verified by the experimental data.

### 2. Structure Composition and working principle

The structure of the contact obstacle detector is shown in Fig. 1, which is composed of a detecting crossbeam, a hanging crossbeam, an integrated box and a support structure. The whole structure is connected with the Metro Bogie and is fixed at the front end of the locomotive through the transition support. The detection crossbeam is designed as an extrapolated structure with inclined plane angle, which makes the obstacles push out of the track, the detection crossbeam and the integrated box are fixed by rack and Bogie, and the impact load is transmitted longitudinally

The integrated box is composed of plate spring, limit switch, adjusting rack and so on. It is designed as a sealing device for dust-proof and water-proof.

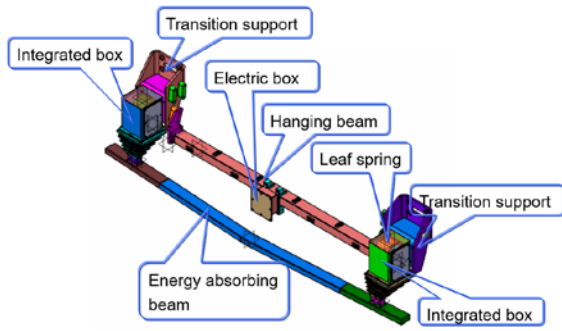


Fig. 1 Structure of obstacle for subway

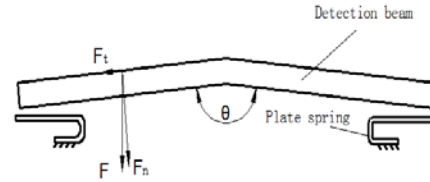


Fig. 2 force analysis of detection beam

During the operation of the subway, when there are no obstacles in front, the contact signal is normal and the vehicle runs safely; when the detector contacts the obstacles, they are lighter, and the mechanism pushes away the obstacles, and the obstacles touch the vehicle to run safely; the obstacles are larger, the trip switch is triggered to protect the Bogie and the vehicle has already triggered the emergency brake, with the front crossmember disconnecting from the larger obstacle.

When a subway hits an obstacle with mass of  $m$ , at speed  $v$ , the normal and tangential forces on the inclined plane (shown in Fig 2) are respectively  $F_n = mv \cos \theta$ ,  $F_t = mv \sin \theta$ . The inclination angle of the detecting crossbeam should be between  $\arctan \mu$  and  $\pi$ . And it will ensure that the tangential component force is greater than the maximum static friction force.

The impact load of the obstacles on the crossbeam will be transmitted longitudinally through the meshing tooth plate, and the plate spring will deform. When deformation exceeds the predetermined value, the trip switch will be triggered to make the vehicle brake emergency, thus ensuring the safety of driving. Obviously, it is the key to design the detector to study and obtain the load-deformation law of the abnormality leaf spring.

### 3. Stiffness Model of Abnormity Leaf Spring

#### 3.1. Structural Mechanics Model of Abnormity Leaf Spring

According to the theory of bending deformation [9], when a beam is subjected to a concentrated load perpendicular to its axis, it will bend and deform. Its bending rigidity can be expressed as:

$$K = E \cdot I_z \quad (1)$$

Where  $e$  is the elastic modulus of the material and  $I_z$  is the moment of inertia of the beam section relative to the  $z$  axis, then  $I_z$  can be expressed as:

$$I_z = \int y^2 dA \quad (2)$$

As shown in figure 3, if the cross-section is rectangular and the length of the rectangle is  $b$  and the width is  $h$ , the moment of inertia of the cross-section relative to the  $Z$ -axis can be expressed as:

$$I_z = \frac{1}{12}bh^3 \quad (3)$$

The deformation of beams with different restraint forms is different when they bear different loads perpendicular to the length of the beam. The most concerned in this paper is the maximum deformation of the  $a$ -end which is in contact with the detection beam [10]. Combined with engineering practice, the effect of deformation superimposition of fillet and joint can be neglected, The stiffness of the tapered section  $BC$  is equivalent to that of the fixed section, so the mechanical model is simplified as a stepped cantilever beam model with a fixed end and a concentrated load at a end (as shown in Fig. 3(b)).

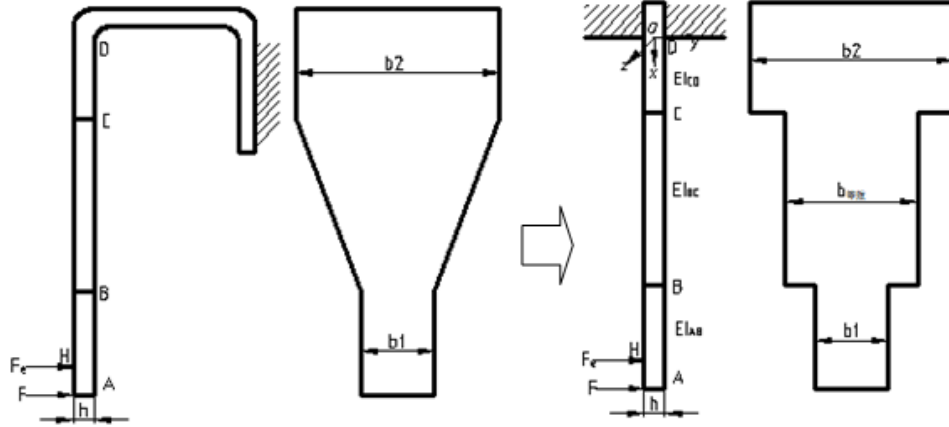


Fig. (a) original mechanical model

Fig. (b) equivalent mechanical model

Fig. 3 structural mechanics model of abnormality leaf spring

### 3.2. Calculation of equivalent fixed section about BC

We assume that the C end is the fixed end, the B end is the applied load  $F$ , the width and cross-sectional moment of inertia at any distance  $x$  from the C terminal can be expressed as:

$$b(x) = b_2 - \frac{b_2 - b_1}{l_{BC}} x \quad (4)$$

$$I_z = \frac{1}{12} \left[ b_2 - \frac{b_2 - b_1}{l_{BC}} x \right] h^3 = I_{CD} \left[ \frac{l_{BC} + (\beta - 1)x}{l_{BC}} \right] \quad (5)$$

$I_{CD}$  is the cross-sectional moment of inertia of the CD segment,  $\beta = \frac{b_1}{b_2}$  is the shape factor.

Introducing equivalent stiffness, according to the same principle of the bending strain energy, the following results are obtained:

$$\frac{1}{2} \int_{l_{BC}} EI_z (y'')^2 dx = \frac{1}{2} \int_{l_{BC}} EI_{BC} (y'')^2 dx \quad (6)$$

The approximate deflection curve equation of the cantilever beam is:

$$y = a \left( x^2 - \frac{x^4}{6l^2} \right) \quad (7)$$

$$y'' = 2a \frac{l^2 - x^2}{l^2} \quad (8)$$

The equivalent stiffness of BC can be obtained by taking the upper formula into (6), Can Be expressed as:

$$EI_{BC} = E \frac{16 + 5(\beta - 1)}{16} I_{CD} \quad (9)$$

According to formulas (9) and (3), the variable section of the BC can be equivalent to the fixed rectangular section of length  $b_e = \frac{16 + 5(\beta - 1)}{16} b_2$  and width  $H$ , so the mechanical model of the abnormality leaf spring structure can be simplified as shown in Fig. 3(b).

## 4. Deformation Calculation of Leaf Spring

### 4.1. Deformation and deformation potential energy of AB segment leaf spring

The calculation of the deformation of the AB segment plate spring can assume that the B end is fixed, the A end is free, and the concentrated load  $F$  acts on A. The imaginary load  $F_e$  is applied at any distance  $x$  from the B end. Bending moment of AH Segment  $M_1$  and HB Segment  $M_2$  can be expressed as:

$$M_1 = F(l_{AB} - x)$$

$$M_2 = F_e(l_{HB} - x) + F(l_{AB} - x)$$

According to the principle of energy [11], the bending deformation of the AB segment of the leaf spring can be as follows:

$$U_{AB} = \frac{1}{2EI_{AB}} \int_0^{l_{HB}} [F_e(l_{HB} - x) + F(l_{AB} - x)]^2 dx + \frac{1}{2EI_{AB}} \int_{l_{HB}}^{l_{AB}} [F(l_{AB} - x)]^2 dx \quad (10)$$

Take a partial derivative of  $F_e$ , and replace  $F_e = 0$ ,  $l_{HB} = l_{AB}$  to get a segment deformation and rotation angle:

$$f_A^{l_{AB}} = \frac{Fl_{AB}^3}{3EI_{AB}} \quad (11)$$

$$\theta_A = \frac{Fl_{AB}^2}{2EI} \quad (12)$$

### 4.2. Deformation and Deformation Potential Energy of BC Segment Spring

Suppose C is the fixed end and B is the free end. The concentrated load  $F$  and Bending moment  $M_C = F(l_{AB} + l_{BC})$  acts on point B Terminal, Also according to formulas (9) and (11), it can be obtained that the CD segment causes the overall rigid displacement of the AB segment and the angle of rotation of the C end along the load direction, as follows:

$$f_A^{l_{CD}} = \frac{Fl_{CD}^3}{3EI_{CD}} + \frac{F(l_{AB} + l_{BC})l_{CD}^2}{2EI_{CD}} \quad (15)$$

$$\theta_C = \frac{Fl_{CD}^2}{2EI_{CD}} + \frac{F(l_{AB} + l_{BC})l_{CD}}{EI_{CD}} \quad (16)$$

So, a step-plate spring with a fixed D-end, a free-end a is subjected to a load  $F$ , the total deformation at end a can be expressed as:

$$f_{\text{总}} = f_A^{l_{AB}} + (f_A^{l_{BC}} + \theta_B l_{AB}) + (f_A^{l_{CD}} + \theta_C l_{AC}) = kF \quad (17)$$

$k$  is related to the dimension  $l_{AB}$ 、 $l_{BC}$ 、 $l_{CD}$ 、 $b_1$ 、 $b_2$ 、 $h$  and  $b_1$  of the leaf spring. It also shows that the relationship between the longitudinal load and the deformation of the detector depends on the shape and size of the leaf spring.

## 5. Experiment on load-deformation of obstacle detector

### 5.1. Principles of Experimentation

The testing platform of displacement characteristic of obstacle detector includes MTS244.21

hydraulic actuator, computer, displacement sensor, data acquisition instrument, etc. (as shown in figure 4). The principle is as follows: first, the obstacle detector is fixed on two steel beams through the Crossbeam, and is fixed on the steel counterforce plate through the steel beam, the actuator applies a horizontal load at a speed of 1mm/min, and the plate spring deforms under the action of the horizontal load, all the data were collected by TST3816E static strain testing system, and the actuator was unloaded to observe and record whether the leaf spring returned to its original position.



Fig. 4 load-displacement test system

## 5.2. Experimental method

The actuator applies a horizontal load at the position shown in Fig. 5 to detect the deflection of the plate spring due to the transfer of loads, toothed plates, etc. The procedure is as follows:

(1) Initial Position 0: The displacement of the Horizontal actuator is adjusted to 0, and the load, strain and displacement are reduced to 0.

(2) producing displacement: The servo hydraulic actuator is used to slowly exert the displacement, and the loading speed is 1mm/min.

(3) continue displacement to 15mm: continue using servo hydraulic actuator slowly apply displacement, loading speed is 1mm/min, until 15mm, maintain the displacement for 1min.

(4) observe for contact: If the spring plate doesn't touch other parts, continue loading at a speed of 1 mm/min; if contact has been made, press next step directly.

(5) reset: According to the speed of 2 mm/min Reset, after returning to the initial position to observe whether the Spring Board returned to the original position, observe and record the state.

Fig. 5 is the input load-displacement curve of the actuator. It can be judged that when the displacement of the actuator is 148 mm, the load reaches a peak value of 7050N; when the displacement is more than 148 mm, the corresponding load of the actuator decreases with the increase of the displacement, it indicates that the leaf spring has entered the yield stage.

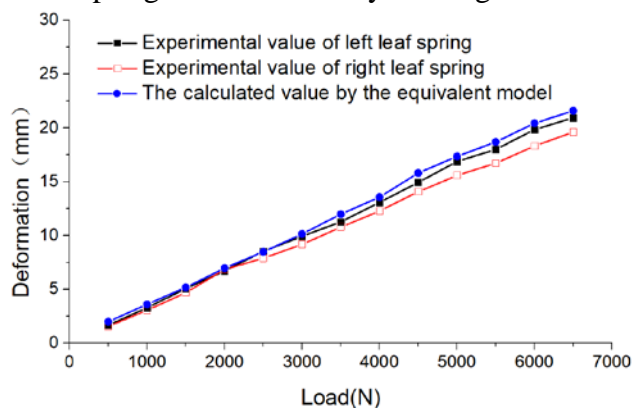
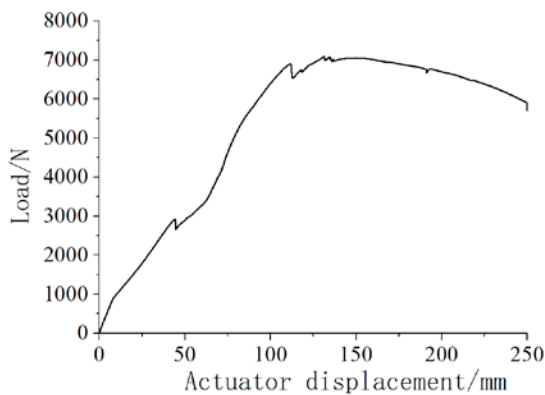


Fig. 5 actuator input displacement-load diagram Fig. 6 load-deformation diagram of leaf spring

## 5.3. Experimental results

At the end of the experiment, the left and right leaf springs could not recover the deformation immediately, and there were 0.90mm and 0.52mm residual deformation respectively. The experimental data of the leaf spring deformation under 0-7000N load are extracted and compared

with the calculated values of the equivalent model, as shown in Fig. 6.

Comparing the calculated results of the equivalent stiffness model of the abnormality leaf spring with the experimental results, the maximum deformation law of the abnormality leaf spring and the measured value increase approximately linearly with the increase of the load, and the maximum error of the two is less than 10% , this shows that the equivalent stiffness model of abnormality leaf spring can be used to evaluate the stiffness of obstacle detection device quickly. During the experiment, when the load is more than 3500N, the growth rate of the measured value of the deformation decreases with the increase of the load.

## 6. Conclusion

In this paper, the structure and working principle of a mechanical contact obstacle removal device are studied, and the longitudinal stiffness of the whole structure is calculated by using the load-maximum deformation of the abnormality leaf spring, a theoretical model of stiffness evaluation based on beam bending theory is established, and then the stiffness evaluation method of the whole structure of the detector is given. The accuracy of the theoretical model is verified by the experimental data, which provides a theoretical reference for the structure design and manufacture .

## Reference

- [1] GAO Qi, SU Chao, LIANG Rujun, et al. (2019) New System Functions for Urban Rail Transit FAO Train and the Design Points. *Urban Mass Transit*, 22(S2),35-38.
- [2] ZHANG Qiang, YANG Feng, ZHANG Bao. (2019) Application Research for Vision-based Train Intelligent Obstacle Detection System Used On Beijing New Airport Express Line. *Railway Locomotive & Car*, 39(06),114-118.
- [3] WANG Wei, LIANG Rujun, HUANG Tao. (2019) Design of Video Recognition System for Subway Train Obstacle. *Urban Mass Transit*, 22(06),166-169.
- [4] FANG Chongquan. (2018) Design of anti-collision warning system for mine locomotive. *Industry and Mine Automation*, 44(09),1-4.
- [5] Liu Shangdong, Wu Ye, JI Yimu, et al. (2019) Research on Security of Key Algorithms in Intelligent Driving System, *Chinese Journal of Electronics*, 28(1), 29-38.
- [6] Song Liangliang, Deng Yongliang, Yuan Jingfeng, et al. (2017) Song Liangliang Deng Yongliang Yuan Jingfeng. *Journal of Southeast University (Natural Science Edition)*, 47(05),1069-1073.
- [7] ZHU Tao, XIAO Shoune, YANG Chao, et al. (2017) State-of-the-art Development of Passive Safety of Rolling Stocks, *Journal of the China Railway Society*, 39(05), 22-32.
- [8] XU Jia, SONG Shou-xin, YUAN Peng-wei, et al. (2015) Evaluation of network vulnerability of subway stations based on ANP. *China Safety Science Journal*, 25(12),129-134.
- [9] GONG Qinghong, MOU Wenping, LUO Jinwei. (2018) Rigid evaluation model for aircraft structural parts web based on beam bending theory. *Manufacturing Technology & Machine Tool*, *Manufacturing Technology & Machine Tool*, (07), 117-123.
- [10]ZHANG Jiawei, SUN Lin, ZHANG Xiangyan, et al. (2019) Effect of initial stresses and deformations on the natural frequencies of beams. *Journal of Vibration and Shock*, 38(02), 46-51.
- [11]HUANG Xiaoming, SUN Jie, LI Jianfeng. (2017) Mathematical Modeling of Aeronautical Monolithic Component Machining Distortion Based on Stiffness and Residual Stress Evolvement. *Journal of Mechanical Engineering*, 53(09), 201-208.